Proceedings of the 21st ICSMGE, Vienna, Austria, 14 – 19 June 2026. Pistrol, Adam & Schweiger (eds.)
Published by: ÖGG, Austrian Society for Geomechanics, Salzburg, Austria, ISBN 978-3-9503898-4-5
https://doi.org/10.53243/ICSMGE2026-223

Greenfield settlements induced by failure of a tunnel involving large displacement

Jianhong Zhang, **Jiaqi Lin**, Aixia Wang
Department of Hydraulic Engineering, State Key Laboratory of Hydroscience and Engineering, Tsinghua University, Beijing, 100084, China, cezhangjh@tsinghua.edu.cn

Xiangsheng Chen
College of Civil and Transportation Engineering, Shenzhen University, Shenzhen, 518060, China

ABSTRACT: Tunneling is a frequently used construction method for underground space development. The construction of new tunnels in cities has great potential to induce deformation in the ground and to damage existing structures and utilities. Many studies have investigated effects of tunnel driving, but failure of tunnel involving large displacement has not been well addressed. The objective of this study is to investigate green-field settlements in a silt induced by failure of a tunnel under construction in a geotechnical centrifuge. The tunnel failure was simulated by lowering a trapdoor 1.8 m downwards. The trapdoor's width characterizes the collapsed width of the tunnel and the associated ground loss. Seven trapdoor tests were conducted, incorporating trapdoor widths of 1, 2, 4, 6, 10, 12 and 16 m. Nine non-contact laser sensor were installed to monitor the settlement of the ground surface. Results of the centrifuge tests indicated that two distinct mechanisms presented in the ground, a curved soil arch formed near the trapdoor at smaller trapdoor widths of 1 – 4 m and a general shear failure occurred at trapdoor widths of 6 – 16 m. Settlements of the greenfield generally conform to standard Gaussian curves and increase nonlinearly with trapdoor width / ground loss. Affected by soil arching, maximum ground settlements were 0.15, 0.18, and 0.2 m for trapdoor widths of 1, 2 and 4 m. When shear failure dominated, the maximum settlements were 0.9, 1.4, 1.7 and 2.1 for trapdoor widths of 6, 10, 12, and 16 m, respectively.

KEYWORDS: Tunnel failure, greenfield settlement, ground loss; centrifuge, deformation.

1 INTRODUCTION

Tunneling is a frequently used construction method for underground space development. When the construction of new tunnels encounters difficult conditions, failure of tunnel support may occur, leading to the collapse of tunnels and inducing large deformation in the ground (Peck, 1969; Mair, 1979; Chang et al., 2001; Farrell, 2010; Ng and Wong, 2013; Ritter, 2017; Huang et al., 2019; Di Mariano et al., 2021). For an example, in 2003, a 238 m – long tunnel, constructed by freezing method, failed at Shanghai Metro Line 4 due to a temperature rise in the freezing equipment (Tan et al., 2021). Another accident happened in 2018 at Guangdong Foshan Metro Line 2, where a 40 m – long shield-driven tunnel collapsed due to leakage at the shield tail (Zhang et al. 2023). These tunnel failure involved significant ground subsidence (Zhang et al., 2025; Lin et al., 2025). Many studies have investigated effects of tunnel driving, but failure of tunnel support system involving large displacement has not been well addressed.

Physical modeling has played an important role in studies related to tunneling. Trapdoor tests, were initially used by Terzaghi (1936) based on small-scale models to explain the arching theory of soil. The tests have been conducted to simulate the response of granular materials to trapdoor displacement. Trapdoor tests under centrifugal conditions have provided insights into arching mechanisms and ground responses induced by tunneling in soft ground (Adachi et al., 1995), as well as in granular soil over active trapdoors (e.g. Burke and Elshafie, 2021). Iglesia et al. (2014) postulated qualitative arching mechanisms evolving from a curved configuration to a triangular shape and ultimately to a prism above a trapdoor at relatively small, intermediate, and large displacements, based on centrifuge modeling of a trapdoor.

The objective of this study is to investigate green-field settlements in a silt induced by failure of a tunnel under construction in a geotechnical centrifuge. The tunnel failure was simulated by lowering a trapdoor 1.8 m downwards. The trapdoor's width characterizes the collapsed width of the tunnel and an associated ground loss. Seven trapdoor widths, i.e. 1, 2, 4, 6, 10, 12 and 16 m were incorporated to examine the effect of the collapsed scope. Nine non-contact laser sensor were installed above the surface of the ground to monitor the settlement of the ground surface. Mechanisms of deformations and failure were observed through a transparent window of the model container using a black and white digital camera placed in front of the window. Effects of the trapdoor width / ground loss and mechanism of soil deformation are discussed..

2 MODEL SETUP AND INSTRUMENT

2.1 *Centrifuge model setup*

Fig. 1 shows a two dimensional greenfield model in a container used for centrifuge trapdoor test. The container had internal dimensions of 0.6 m long × 0.2 m wide × 0.53 m high. A transparent front window enabled visual monitoring during the test.

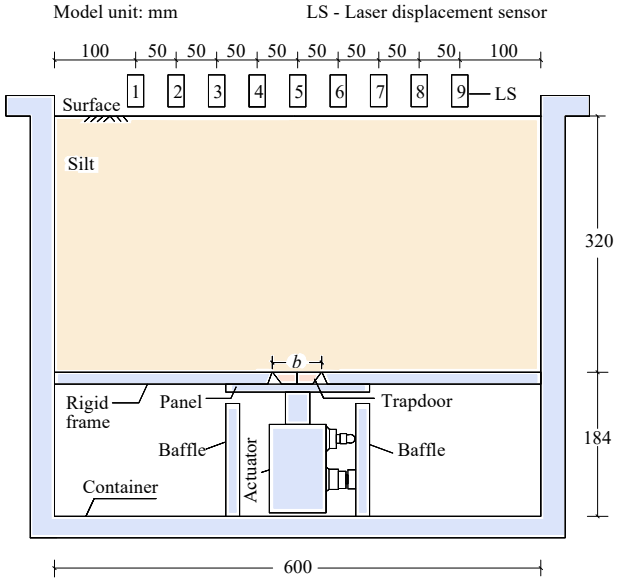

Figure 1. Centrifuge model of greenfield trapdoor test in a silt.

A trapdoor, having a width of *b*, was located under a 320 mm thick silt. The trapdoor was supported by an actuator, simulating a tunnel failure by moving the actuator 18 mm downwards. Seven trapdoor widths, i.e. *b* = 10, 20, 40, 60, 100, 120 and 160 mm were incorporated to examine the effect of failure scope of the tunnel. The moving patterns of the trapdoor, i.e. stable and failure modes, are illustrated in Figure 2. The width of the trapdoor characterized the scope of tunnel failure. The gap formed by the trapdoor's final from its initial position per unit length was denoted as the ground loss ΔV. The ΔV was in approximately linear relationship with *b*, i.e. ΔV = 1.48 *b*, hence, the trapdoor width was considered to represent ΔV.

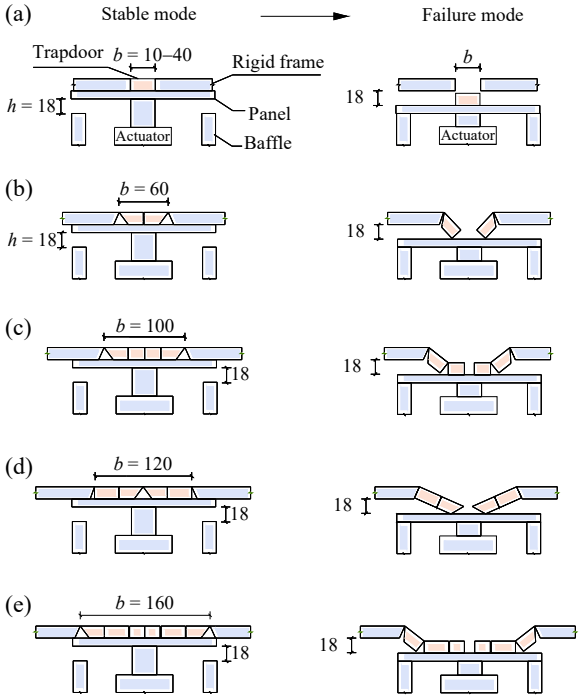

Figure 2. Stable and failure modes of trapdoors with width of: (a) 10, 20 and 40 mm, (b-e) 60 – 160 mm (model unit: mm).

The silt had a plasticity index of 6.5 and a liquid limit of 25%. It was compacted to a dry density of 1500 kg/m^3 at a water content of 6%. Its effective cohesion and friction angle were determined to be 6.1 kPa and 28.9° through consolidated undrained triaxial test (ASTM D 7181). All the models were tested at a centrifugal acceleration of 100 g and were scaled to adhere to the scaling law (Taylor, 1995).

2.2 *Instrument and test procedures*

After the soil compaction, markers were placed on the side of the soil facing a transparent sidewall of the container. A black and white digital camera was positioned in front of the sidewall to capture the movement of the markers and thus analyze deformations of the soil. The trapdoor was lowered 18 mm by moving the actuator down to reproduce the critical condition. An ultimate state of the trapdoor was denoted at *h* = 18 mm. Nine laser sensors were installed above the ground surface to record the greenfield settlements, numbered 1 to 9 from left to right, as shown in Figure 1.

Following preparation, the centrifuge was accelerated from 1 to 100 g and then maintained at 100 g. The trapdoor was lowered by 18 mm in 0.5 seconds when the ground surface settlements stabilized. The model was monitored by a camera at 20 frame/s, while the laser sensors recorded data at 0.05 Hz. The dimensions of the model and the measured deformations were scaled up by a factor of 100 for the prototype in subsequent sections. Results of the tests are presented in a prototype scale in later sections.

3 GREENFIELD SETTLEMENTS

3.1 *Failure mechanism*

The prototype of the centrifuge model was a 32 m deep ground above a tunnel which was susceptible to failure, as depicted in Figure 3. Given the centrifugal acceleration of 100 g at which the models were tested, the width of the failed tunnel was 1, 2, 4, 6, 10, 12, and 16 m in seven models, respectively. The maximum downwards displacement of the trapdoors was identically 1.8 m for all the seven models. Deformation and failure mechanism of the soil were observed to examine its effect on the greenfield settlement.

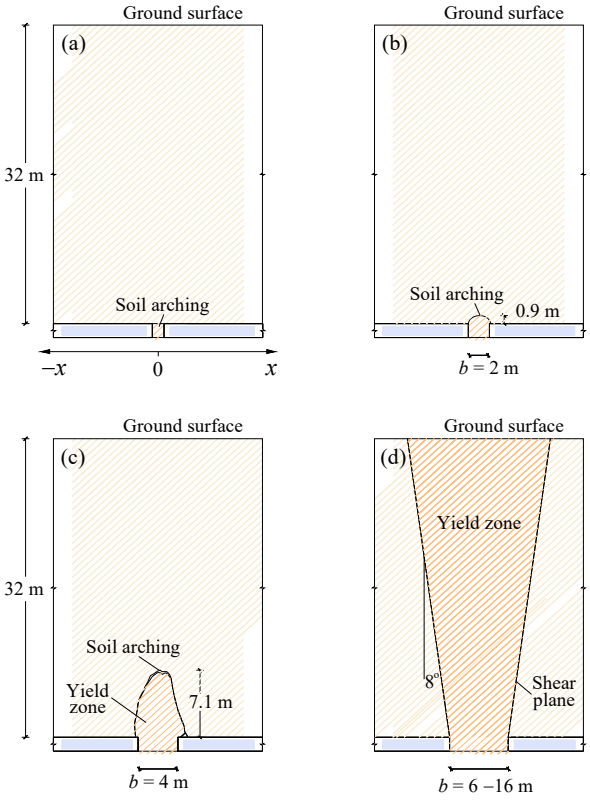

Figure 3. Failure mechanism versus trapdoor width: (a) - (c) Soil arching domanted at *b* = 1, 2, and 4 m; (d) General failure at *b* = 6, 10, 12, and 16 m.

When the trapdoor move down 1.8 m, simulating the tunnel failure, a physical soil arch formed from the edge of the trapdoor, at trapdoor widths of b = 1, 2 and 4 m, as shown in Figures. 3a – 3c. A small yield zone developed due to relative displacements between the trapdoor and the adjacent stable soil. The size of the arch and the yield zone expanded with the trapdoor width. For instance, at *b* = 1 m, the soil arch and q yield zone formed just at the trapdoor (Figure 3a), no upward development at all. When *b* = 2 m, a curved arch appeared above the trapdoor and a yield zone enlarged, having a width over 2 m and a height of 0.9 m (Figure 3b). When the trapdoor width increased to 4 m, the yield zone expanded further to a triangle shape, with a width about 5 m and a height of 7.1 m (Figure 3c). These three cases revealed an arch shape analog to that proposed by Iglesia et al. (2014) for relatively small

trapdoor displacements. It may indicate that small trapdoor width had the same effect as the small trapdoor displacements. Nevertheless, the smaller the width, the easier the soil arch formed. When soil arching effect dominated, ground settlements were found relative small.

When the trapdoor width increased to $b = 6$ m, soil arching first occurred at small trapdoor displacements, e.g. less than 1.0 m, but not sustained when the trapdoor displacement became larger. A potential of general shear failure presented and the yield zone tended to reach the ground surface. When the trapdoor width further increased to 10, 12, and 16 m, arching effect was difficult to observe in the soil. The yield zone further expanded in width, developed upwards and finally extended to the ground surface, leading to a general shear failure. Figure 3d illustrates a failure zone bonded by two shear plane. An angle of draw, δ, about 8 degree to the vertical direction as seen in Figure 3d. Iglesia et al. (2014) proposed a prism failure mechanism for large trapdoor displacements. In this study, a similar mechanism was also found in the soil, but at large trapdoor width. Therefore, the big trapdoor width had the same effect as the large trapdoor displacements. This general shear failure mechanism will then significantly affected the ground settlement.

3.2 *Greenfield settlements*

The above mentioned ground response mechanisms typically led to vertical displacements that tended to develop at the ground surface as tunnel failure proceeded. The magnitude and distribution of surface settlements depend on the deformability of the ground, the ground response mechanism, and the position or distance relative to the trapdoor. Figure 4 provides the time history of the measured surface settlement, *s,* induced by the trapdoor movement, at trapdoor width of 1 m and 6 m.

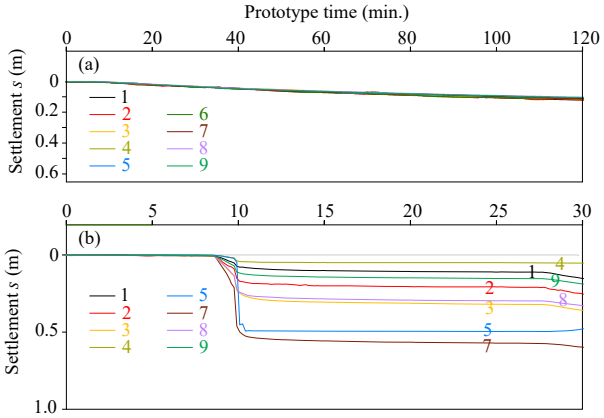

Figure 4. Time history of measured surface settlement at trapdoor width: (a) $b = 1$ m; (b) $b = 6$ m.

Figure 4a shows the results of the test at a trapdoor width of 1 m, in which 1 – 9 were the number of the laser displacement sensors. The settlement increased gradually with time or ground loss. As only a small yield zone appeared at the trapdoor, the resulted surface settlement was quite insignificant, compared to the trapdoor displacement of 1.8 m. A maximum value of 0.15 m occurred above the centerline of the trapdoor, i.e. at x = 0, x is the distance from the centerline of the trapdoor. As seen in Figs. 3a-3c, soil arching mechanism dominated in the three models with trapdoor width of 1, 2, and 4 m. The arching mechanism led to similar situations, i.e. relative small surface settlements, with maximum values of 0.15, 0.18, and 0.2 m for the models with trapdoor width of 1, 2, and 4 m, respectively.

In contrary, when the trapdoor width increased to 6 m, a general shear failure began to dominate. The angle of draw, δ, about 8 degree in Figure 3d, defines the practical extent of surface subsidence or the maximum settlement, s_{max} at $x = 0$. The mechanism thus induced greater settlements, as illustrated in Figure 4b at a trapdoor width of 6 m. A maximum settlement of 0.9 m was found above the trapdoor, much higher than those in previous models, indicating a strong effect of the failure mechanism. When the trapdoor width further increased to 10, 12, and 16 m, the mechanism of general shear failure dominated, more significant settlements were found in the models, with maximum values of 1.4, 1.7, and 2.6 m, respectively.

Subsurface ground movements were also measured through tracing markers placed in the soil. Figure 6 depicts the settlement versus soil depth for the model with trapdoor width of 6 m before the general shear failure of the soil. Due to soil dilation, the settlement decreased from the trapdoor where the yield zone initiated.

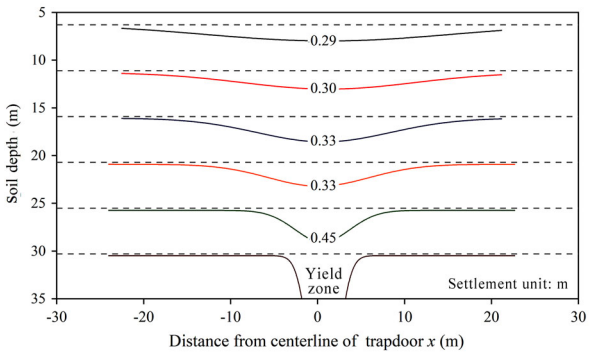

Figure 5. Settlements versus soil depth at trapdoor width of 6 m.

The settlements at the ground surface resulted in what is referred to as the settlement trough. For practical purposes, the observed two-dimensional trough is conventionally characterized along the trapdoor centerline. To describe the trough shape, Figure 6 depicts the settlement, s, at various distances x from the trapdoor's centerline. A standard Gaussian curve was used to fit the measured data for the seven greenfield models. As seen in Figure 6, the ground settlements typically follow a standard Gaussian curve (Marshall et al., 2012; Franza et al., 2015), with the maximum settlement, smax, and the trough shape parameter, i, the horizontal distance of the inflection point, defining the shape of the curve.

$$s = s_{max} exp\left(-\frac{x^2}{2i^2}\right) \quad (1)$$

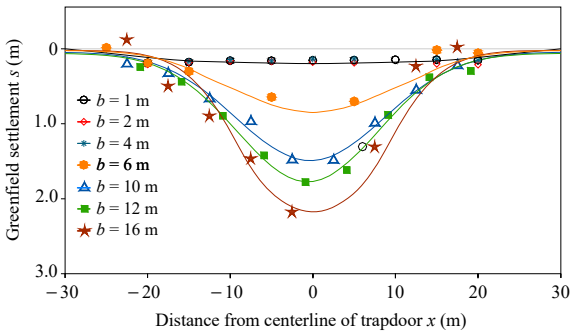

Figure 6. Measured greenfield settlements and Gaussian curve fittings at seven trapdoor widths.

Based on Equation 1, the maximum settlements s_{max} are 0.15, 0.18, 0.2, 0.9, 1.4, 1.7, and 2.1 m at trapdoor widths of 1, 2, 4, 6, 10, 12, and 16 m, respectively. This increase in the maximum settlement nonlinearly correlates with the trapdoor width, as depicted in Figure 7. There is a two phase trend, i.e. a flat phase reflecting the soil arching effect, then a rapid growth displaying the effect of the general failure. Table 1 summarizes parameters of the curve fitting. The trough shape parameters, i, ranges between 8.0 – 8.5, giving an average of 8.5, so the half-width of the settlement trough is about 2.8 i. Previous studies indicated that i is approximately a linear function of the tunnel depth (Z_0) (O'Reilly and New, 1982), expressed as follows:

$$i = KZ_0 \quad (2)$$

where K is the trough width parameter, which can be taken as 0.4 for stiff clay, 0.7 for soft and silty clay, and 0.2 – 0.3 for granular material. In this study, Z_0 is 32 m, and the average i is 8.5 m, so K is 0.27, belonging to the category of granular material.

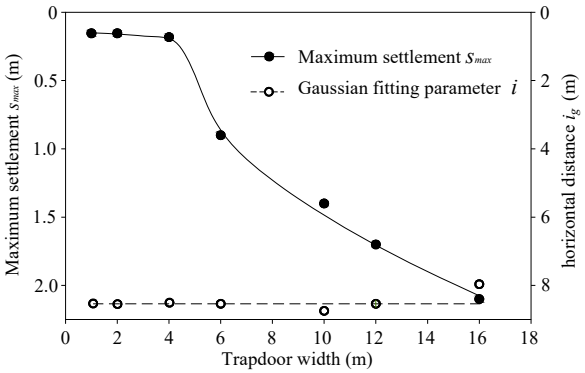

Figure 7. Maximum settlement and horizontal distance of the inflection point versus trapdoor width.

Table 1. Ground settlement at different trapdoor width

Trapdoor width (m)	Maximum settlement (m)	Trough shape parameter i (m)
1	0.15	8.5
2	0.18	8.5
4	0.2	8.5
6	0.9	8.5
10	1.4	8.7
12	1.7	8.5
16	2.1	8.0

4 CONCLUSIONS

This centrifuge study investigates the greenfield responses in silt to the failure of a tunnel simulated by a trapdoor.The physical investigation led to the following conclusions:

a. Physical soil arch formed at small trapdoor widths of 1 – 4 m, developing from the edge of the trapdoor. It resulted in small settlements of 0.15, 0.18, and 0.2 m for trapdoor widths of 1, 2, and 4 m, respectively.

b. General shear failure occurred at 6 − 16 m trapdoor, extending to the ground surface. Significant settlements of 0.9, 1.4, 1.7, and 2.1 m were induced for trapdoor of 6, 10, 12, and 16 m, respectively.

c. The greenfield settlements generally conform to standard Gaussian curves and nonlinearly increase with the ground loss or trapdoor width.

5 ACKNOWLEDGEMENTS

This work was supported by the National Natural Science Foundation of China under Grant No. 52279101, 52090084, and 52494971.

6 REFERENCES

Adachi, T., Tamura, T., Kimura, K., and Nishimura. T. 1995. Axial symmetric trap door tests on sand and cohesion soil. Proceedings of the 30th Japan National Conference on Geotechnical Engineering, 1973–1976 (in Japanese).

Burke, T.S., and Elshafie, M.Z.E.B. 2021. Arching in granular soils: experimental observations of deformation mechanisms. Géotechnique 71(10): 866–878.

Chang, C.T., Sun, C.W., Duann, S.W., and Hwang. R.N. 2001. Response of a Taipei Rapid Transit System (TRTS) tunnel to adjacent excavation. Tunneling and Underground Space Technology 16 (3), 151–158.

Di Mariano, A., Varga, A. and Gens. A. 2021. An underground excavation in Barcelona and its interaction with existing structures. Geotechnical Aspects of Underground Construction in Soft Ground, Elshafie, Viggiani and Mair (eds.) ISSMGE, London, UK, 536–544.

Farrell, R. 2010. Tunnelling in sands and the response of buildings. PhD thesis, Cambridge University, Cambridge, UK.

Franza, A., and Marshall. A.M. 2015. Analytical investigation of soil deformation patterns above tunnels in sandy soil. Proceedings of XVI ECSMGE geotechnical engineering for infrastructure and development, Edinburgh, 467–472.

Huang, M. S., Zhou, X.C., Yu, J., Leung, C.F., and Tan. J.Q.W. 2019. Estimating the effects of tunnelling on existing jointed pipelines based on Winkler model. Tunnelling and Underground Space Technology 86, 89–99.

Iglesia, G. R., Einstein, H.H., and Whitman, R.V. 2014. Investigation of soil arching with centrifuge tests. Journal of Geotechnical and Geoenvironmental Engineering 140 (2), 04013005.

Lin, J.Q., Zhang, J.H., Wang, A.X., and Chen, X.S. 2025. Strain responses of an existing tunnel to instability of a new tunnel. Geotech Asia Conference 2025, Oct. 7-10. Goa, India.

Marshall, A.M., Farrell, R., Klar, A., & Mair, R. 2012. Tunnels in sands: the effect of size, depth and volume loss on greenfield displacements. Géotechnique 62(5), 385–399.

Mair, R.J. 1979. Centrifugal modelling of tunnel construction in soft clay. Ph.D. thesis, University of Cambridge.

Ng, C.W.W., and Wong, K.S. 2013. Investigation of passive failure and deformation mechanisms due to tunnelling in clay. Canadian Geotechnical Journal 50, 359–372.

O'Reilly, M.P., and New, B.M. 1982. Settlements above tunnels in the United Kingdom – their magnitude and prediction. Tunnelling 173–181. London: IMM.

Peck, R.B. 1969. Deep excavations and tunneling in soft ground. Proceedings of the Seventh International Conference on Soil Mechanics and Foundation Engineering. Mexico City, 225– 290.

Ritter, S. 2017. Experiments in tunnel–soil–structure interaction. PhD thesis, University of Cambridge, Cambridge, UK,

Tan, Y., Lu, Y., and Wang, D.L. 2021. Catastrophic Failure of Shanghai Metro Line 4 in July, 2003: Occurrence, Emergency Response, and Disaster Relief. Journal of Performance Construction Facility, 2021, 35, 04020125.

Taylor, R.N. 1995. Geotechnical centrifuge technology. Blackie Academic and Professional, London.

Terzaghi, K. 1936. Stress distribution in dry and in saturated sand above a yielding trap–door. Proceedings of the International Conference on Soil Mechanics, Harvard University. Press, Cambridge, MA, vol. 1. 307–311.

Zhang, J.H., Wang, A.X., Zhang, L.M., and Chen, X.S. 2023. Coupling failure mechanism of underground structures induced by construction disturbances, Mathematics 2023, 11, 615.

Zhang, J.H., Wang, A.X., and Chen, X.S. 2025. Deformation and strain mechanisms of an existing tunnel subject to failure of a new tunnel, International Journal of Geotechnical Engineering 19(4), 147-157.